Energy Detection of Primary Signals over $\eta - \mu$ Fading Channels

Saman Atapattu, Chintha Tellambura, and Hai Jiang
Department of Electrical and Computer Engineering, University of Alberta, Edmonton, AB, Canada
Email: {atapattu, chintha, hai.jiang}@ece.ualberta.ca

***Abstract*—In this paper[1], the performance analysis of an energy detector is exploited under the $\eta-\mu$ fading channel model. The received unknown signal at the energy detector is considered as the primary signal transmitted by a primary network user (e.g. cognitive radio network). This research is focused on derivation of the closed-form average detection probability over the $\eta - \mu$ fading channel model. Further, results are extended to two diversity reception cases such as maximal ratio combining (MRC) and square-law combining (SLC) techniques with independent fading channels. Detection performance is discussed with receiver operating characteristics (ROC) curves. Our analysis is validated by numerical and simulation results.**

***Index Terms*—$\eta - \mu$ fading model, diversity, energy detection.**

I. Introduction

Currently, there is an increasing interest of energy detection of unknown signals. As an obvious example, detection of primary user signals is one of the key challenges in cognitive radio networks. Due to the spectrum scarcity in wireless networks, low-priority secondary users try to access the spectrum of primary users (licensed users) once the primary users are sensed to be idle over their allocated spectrum band [1], [2], [3], [4]. This kind of spectrum sensing can be done with a matched filter, a cyclostationary feature detector, or an energy detector [5].

Since the energy detector is non-coherent type with low implementation complexity, it is a popular method which has been analyzed in the literature. An energy detector measures the received signal energy and compares it with a pre-defined threshold to determine the presence or absence of an unknown signal in wireless communication networks. Further, applications of the energy detector is widely used in ultra-wideband (UWB) communications to borrow an idle channel from authorized users [6].

Detection probability (P_d), false alarm probability (P_f) and missed detection probability ($P_m = 1 - P_d$) are the key measurement metrics that are used to discuss the performance of an energy detector. In conventional studies, performance of an energy detector is illustrated by the receiver operating characteristics (ROC) curve which is a plot of P_d versus P_f or P_m versus P_f. The detection of an unknown deterministic signal in the presence of additive white Gaussian noise (AWGN) is analytically formulated in [7] for a flat and band-limited Gaussian channel. Based on the results in [7], P_d and P_f have been derived in closed-form over AWGN channel in [9]. The ROC analysis for Rayleigh, Rice and Nakagami fading channels is discussed in [8] and [9] as two independent works with different analytical approaches. Further, energy detection under different diversity receptions such as maximal ratio combining (MRC), selection combining (SC), switch-and-stay combining (SSC), square-law combining (SLC), square-law selection (SLS) and equal gain combining (EGC) is analyzed in [9], [10], [11]. Detection performance of an energy detector is investigated in [12] for relay-based cognitive radio networks in order to sense the "white spaces" in the spectrum cooperatively. Considering the multipath fading and the shadowing effect, signal detection is analyzed for K and K_G fading models in [13]. In [14], area under the ROC curve (AUC) is introduced as a simpler performance measure of the overall detection capability of the energy detector.

The $\eta - \mu$ distribution is a more general physical fading model because it can represent one-sided Gaussian, Rayleigh, Nakagami-m and Hoyt (Nakagami-q) distributions by changing the parameters η and μ [15], [16]. However, performance of digital communication systems over η-μ fading channel has not been investigated widely in wireless networks. In this paper, we analyze the performance of an energy detector under the $\eta - \mu$ fading channel. The average detection probabilities are derived in closed-form, for cases without diversity reception and with diversity reception such as MRC and SLC. Moment generating function (MGF) approach is applied to evaluate P_d. Further, the Residue Theorem is used to solve the contour integration in the expression of P_d.

The rest of the paper is organized as follows. The system model and the channel model are described in Section II. Average detection problem of the energy detector is analyzed in Section III and Section IV for cases without diversity reception and with diversity reception, respectively. The numerical and simulation results are presented in Section V. The concluding remarks are made in Section VI.

II. System Model

In general, the received signal at time t, $y(t)$ at the wireless receiver can simply be expressed as $y(t) = c{\cdot}s(t)+n(t)$, where c, $s(t)$ and $n(t)$ are channel coefficient between transmitter and receiver, transmitted signal and AWGN with single-sided power spectral density N_0 at the receiver, respectively. When there is no signal from the transmitter, the receiver receives

[1]This research was supported by the Gangwon-Alberta Research Collaboration Fund, the Natural Science and Engineering Research Council (NSERC) of Canada, and the Alberta Ingenuity Fund (AIF), Alberta, Canada.

978-1-4244-4837-1/09/$25.00 ©2009 Crown

noise signal only, which is denoted as hypothesis $\mathcal{H}_0$. Otherwise, the receiver receives both signal and noise, which is denoted as hypothesis $\mathcal{H}_1$. Therefore, the received signal at the receiver can be interpreted as a binary hypothesis:

$$y(t) = \begin{cases} n(t) & : \mathcal{H}_0, \\ c \cdot s(t) + n(t) & : \mathcal{H}_1. \end{cases} \tag{1}$$

A. Fading Channel Model

The η-μ fading channel model is a generalized channel representation to model the non-line of sight small-scale fading such as Rayleigh, Nakagami-m and Hoyt (Nakagami-q) distributions. The probability density function (PDF) of the normalized fading envelop, X, can be written as [16]

$$f_X(x) = \frac{4\sqrt{\pi}\mu^{\mu+\frac{1}{2}}h^{\mu}}{\Gamma(\mu)H^{\mu-\frac{1}{2}}} x^{2\mu} e^{-2\mu h x^2} I_{\mu-\frac{1}{2}}\left(2\mu H x^2\right) \tag{2}$$

where the parameter $\mu = \frac{\mathbb{E}^2(X^2)}{2Var(X^2)}\left(1+\frac{H^2}{h^2}\right)$ represents the number of multipath clusters ($\mu > 0$), $\Gamma(\cdot)$ is the gamma function, and $I_v(\cdot)$ is the v^{th} order modified Bessel function of the first kind. Here $\mathbb{E}(\cdot)$ and $Var(\cdot)$ represent mathematical expectation and variance, respectively. The η-μ fading channel includes two different physical representations as Format 1 and Format 2. The parameters H, h and η are defined for both formats as follows.

1) Format 1: Independent in-phase and quadrature components of the fading coefficient have different powers. And η is the power ratio, $0 < \eta < \infty$. The respective H and h are defined as

$$H = \frac{\eta^{-1} - \eta}{4} \quad \text{and} \quad h = \frac{2 + \eta^{-1} + \eta}{4}.$$

2) Format 2: Correlated in-phase and quadrature components of the fading coefficient have identical powers. And η is the correlation coefficient, $-1 < \eta < 1$. The respective H and h are defined as

$$H = \frac{\eta}{1-\eta^2} \quad \text{and} \quad h = \frac{1}{1-\eta^2}.$$

B. Signal-to-Noise Ratio (SNR)

The received instantaneous signal-to-noise ratio (SNR), denoted γ, is the key measurement of the digital wireless communication networks. The PDF of SNR under the $\eta - \mu$ fading model is given by [16]

$$f_\gamma(x) = \frac{2\sqrt{\pi}\mu^{\mu+\frac{1}{2}}h^{\mu}}{\Gamma(\mu)H^{\mu-\frac{1}{2}}\bar{\gamma}^{\mu+\frac{1}{2}}} x^{\mu-\frac{1}{2}} e^{\frac{-2\mu h x}{\bar{\gamma}}} I_{\mu-\frac{1}{2}}\left(\frac{2\mu H x}{\bar{\gamma}}\right) \tag{3}$$

where $\bar{\gamma}$ is the average SNR of the fading channel.

The moment generating function (MGF) of γ, $M_\gamma(s) = \mathbb{E}(e^{-s\gamma})$, is given by [17]

$$M_\gamma(s) = \left(\frac{K}{(s+c_1)(s+c_2)}\right)^{\mu} \tag{4}$$

where $K = \frac{4\mu^2 h}{\bar{\gamma}^2}$, $c_1 = \frac{2(h-H)\mu}{\bar{\gamma}}$ and $c_2 = \frac{2(h+H)\mu}{\bar{\gamma}}$.

III. Detection Analysis

In this section, we derive the closed-form average detection probability for an energy detector under the $\eta - \mu$ fading channel model.

A. Energy Detector

As described in [7], [9], the received signal is first filtered with a bandpass filter in bandwidth W to normalize the noise variance and to limit the noise power. The output signal is then squared and integrated as follows: for each in-phase or quadrature component, a number u of samples over a time interval T are squared and summed. The summation results of the in-phase component and quadrature component are added together, which yields the test statistic, denoted Y. The PDF of the test statistic, $f_Y(y)$, follows a central chi-square distribution under $\mathcal{H}_0$, and a noncentral chi-square distribution under $\mathcal{H}_1$, given by [9]

$$f_Y(y) = \begin{cases} \frac{1}{2^u\Gamma(u)} y^{u-1} e^{-\frac{y}{2}} & : \mathcal{H}_0, \\ \frac{1}{2}\left(\frac{y}{2\gamma}\right)^{\frac{u-1}{2}} e^{-\frac{2\gamma+y}{2}} I_{u-1}(\sqrt{2\gamma y}) & : \mathcal{H}_1. \end{cases} \tag{5}$$

Note that u is an integer equal to TW or $(TW+1)$. The test statistic Y is compared with a predefined threshold value λ at the receiver. The probabilities of false alarm (P_f) and detection (P_d) can be generally evaluated by $Pr(Y > \lambda|\mathcal{H}_0)$ and $Pr(Y > \lambda|\mathcal{H}_1)$ respectively to yield [9]

$$P_f = \frac{\Gamma(u, \frac{\lambda}{2})}{\Gamma(u)} \tag{6}$$

and

$$P_d = Q_u(\sqrt{2\gamma}, \sqrt{\lambda}), \tag{7}$$

where $Q_u(\cdot,\cdot)$ is the generalized Marcum-Q function and $\Gamma(\cdot,\cdot)$ is the upper incomplete gamma function which is defined by the integral form $\Gamma(a,x) = \int_x^\infty t^{a-1}e^{-t}dt$ and $\Gamma(a,0) = \Gamma(a)$. Probability of false alarm P_f can easily be calculated using (6). Therefore, our focus in the following is on the detection probability.

B. Average Detection Probability

Average detection probability can be found by averaging (7) by SNR distribution $f_\gamma(x)$ in (3). However, it is difficult to find a closed-form solution for direct integration of the generalized Marcum-Q function. Therefore, we use an alternative method which is also used in [12]. The generalized Marcum-Q function can be written as a circular contour integral within the contour radius $r \in [0,1)$. Therefore, expression (7) can be re-written [18] as

$$P_d = \frac{e^{-\frac{\lambda}{2}}}{j2\pi} \oint_C \frac{e^{(\frac{1}{z}-1)\gamma + \frac{\lambda}{2}z}}{z^u(1-z)} dz, \tag{8}$$

where C is a circular contour of radius $r \in [0,1)$. Then, the average detection probability is

$$\begin{aligned}\overline{P_d} &= \int_0^\infty P_d f_\gamma(x)dx \\ &= \frac{e^{-\frac{\lambda}{2}}}{j2\pi}\oint_C \left(\int_0^\infty e^{(\frac{1}{z}-1)x} f_\gamma(x)dx\right)\frac{e^{\frac{\lambda}{2}z}}{z^u(1-z)}dz \\ &= \frac{e^{-\frac{\lambda}{2}}}{j2\pi}\oint_C M_\gamma\left(1-\frac{1}{z}\right)\frac{e^{\frac{\lambda}{2}z}}{z^u(1-z)}dz. \end{aligned} \tag{9}$$

where the last equality comes from the fact that $M_\gamma\left(1-\frac{1}{z}\right) = \int_0^\infty e^{(\frac{1}{z}-1)x} f_\gamma(x)dx$.

Since the MGF of the η-μ channel is known (as given in (4)), the average detection probability can be re-written as

$$\overline{P_d} = \left(\frac{K}{(1+c_1)(1+c_2)}\right)^\mu \frac{e^{-\frac{\lambda}{2}}}{j2\pi}\oint_C g(z)dz, \tag{10}$$

where $g(z) = \frac{e^{\frac{\lambda}{2}z}}{z^{u-2\mu}(1-z)\left(z-\frac{1}{1+c_1}\right)^\mu\left(z-\frac{1}{1+c_2}\right)^\mu}$.

The Residue Theorem [19] shows that the solution of a contour integral with a closed contour in the complex plane can be evaluated with the residues of the integrand. Therefore, $\overline{P_d}$ in (10) can be calculated from the residues of $g(z)$ within the contour radius $r \in [0,1)$. Two cases need to be considered. Note that we consider μ to be an integer.

1) When $u > 2\mu$: There are $(u-2\mu)$ poles at origin, μ poles at $\frac{1}{1+c_1}$ and μ poles at $\frac{1}{1+c_2}$ in radius $r \in [0,1)$. Therefore, $\overline{P_d}$ can be derived as

$$\begin{aligned}\overline{P_d} =& e^{-\frac{\lambda}{2}}\left(\frac{K}{(1+c_1)(1+c_2)}\right)^\mu \\ &\cdot\left(\text{Res}\,(g;0) + \text{Res}\big(g;\frac{1}{1+c_1}\big) + \text{Res}\big(g;\frac{1}{1+c_2}\big)\right)\end{aligned} \tag{11}$$

where $\text{Res}\,(g;0)$, $\text{Res}\big(g;\frac{1}{1+c_1}\big)$ and $\text{Res}\big(g;\frac{1}{1+c_2}\big)$ denote the residue of the function $g(z)$ at origin, $\frac{1}{1+c_1}$ and $\frac{1}{1+c_2}$, respectively. Each residue can be calculated as

$$\begin{aligned}\text{Res}\,(g;0) =& \frac{1}{(u-2\mu-1)!} \\ &\cdot\left[\frac{d^{u-2\mu-1}}{dz^{u-2\mu-1}}\frac{e^{\frac{\lambda z}{2}}}{(1-z)\prod_{i=1}^2\left(z-\frac{1}{1+c_i}\right)^\mu}\right]\Bigg|_{z=0},\end{aligned} \tag{12}$$

$$\begin{aligned}\text{Res}\big(g;\frac{1}{1+c_1}\big) =& \frac{1}{(\mu-1)!} \\ &\cdot\left[\frac{d^{\mu-1}}{dz^{\mu-1}}\frac{e^{\frac{\lambda z}{2}}}{(1-z)z^{u-2\mu}\left(z-\frac{1}{1+c_2}\right)^\mu}\right]\Bigg|_{z=\frac{1}{1+c_1}}\end{aligned} \tag{13}$$

and

$$\begin{aligned}\text{Res}\big(g;\frac{1}{1+c_2}\big) =& \frac{1}{(\mu-1)!} \\ &\cdot\left[\frac{d^{\mu-1}}{dz^{\mu-1}}\frac{e^{\frac{\lambda z}{2}}}{(1-z)z^{u-2\mu}\left(z-\frac{1}{1+c_1}\right)^\mu}\right]\Bigg|_{z=\frac{1}{1+c_2}}.\end{aligned} \tag{14}$$

2) When $u \le 2\mu$: There are μ poles at $\frac{1}{1+c_1}$ and μ poles at $\frac{1}{1+c_2}$ in radius $r \in [0,1)$. Therefore, $\overline{P_d}$ can be derived as

$$\begin{aligned}\overline{P_d} =& e^{-\frac{\lambda}{2}}\left(\frac{K}{(1+c_1)(1+c_2)}\right)^\mu \\ &\cdot\left(\text{Res}\big(g;\frac{1}{1+c_1}\big) + \text{Res}\big(g;\frac{1}{1+c_2}\big)\right).\end{aligned} \tag{15}$$

$\text{Res}\big(g;\frac{1}{1+c_i}\big)$ for $i=1,2$ can be calculated as (13) and (14).

IV. Diversity Reception

A. Maximal Ratio Combining (MRC)

We consider an L branches MRC. Each diversity branch is multiplied by the weighting factor which is proportional to its complex fading coefficient. The instantaneous SNR at the output of the L-branch combiner is

$$\gamma^{MRC} = \sum_{i=1}^L \gamma_i$$

where γ_i is the instantaneous SNR of ith branch. Since square-and-integrate operation of the energy detector is done after combining, the probabilities of false alarm and detection can be derived after replacing γ by γ^{MRC} in (6) and (7), respectively. Further, for independent and identical diversity branches, MGF of γ^{MRC}, $M_{\gamma^{MRC}}(s)$, can be written as

$$M_{\gamma^{MRC}}(s) = \Big[M_\gamma(s)\Big]^L.$$

Therefore, average detection probability under MRC reception, $\overline{P_d^{MRC}}$, can be evaluated after replacing μ by $L\mu$ in (10).

B. Square-Law Combining (SLC)

We consider an L branches SLC. Each diversity branch undergoes square-and-integrate operation before combining. Therefore, decision is based on L independent statistics. Further, the instantaneous SNR at the output of the L-branch combiner is $\gamma^{SLC} = \sum_{i=1}^L \gamma_i$. The corresponding probabilities of false alarm and detection in (6) and (7) can be written as

$$P_f = \frac{\Gamma(Lu,\frac{\lambda}{2})}{\Gamma(Lu)} \quad \text{and} \quad P_d = Q_{Lu}(\sqrt{2\gamma^{SLC}},\sqrt{\lambda}),$$

respectively. For independent and identical diversity branches, MGF of γ^{SLC} can be written as $M_{\gamma^{SLC}}(s) = \Big[M_\gamma(s)\Big]^L$ which has similar form as $M_{\gamma^{MRC}}(s)$. The average detection probability under SLC reception, $\overline{P_d^{SLC}}$, can be evaluated after replacing μ by $L\mu$ and u by Lu in (10).

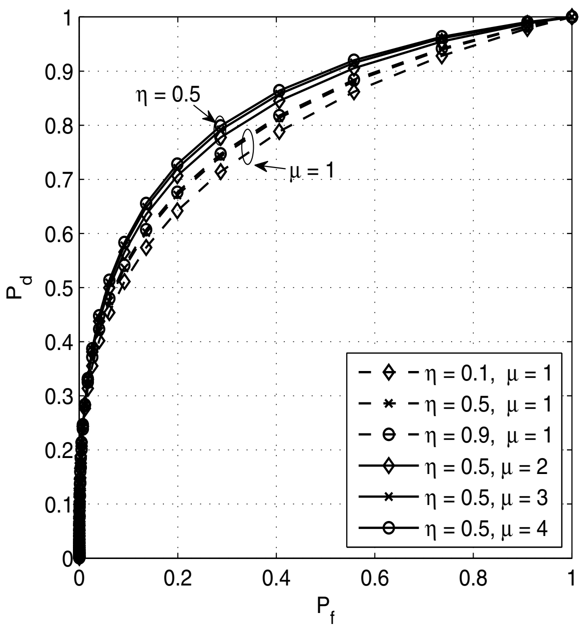

Fig. 1. P_d versus P_f for Format 1 with different η and μ values.

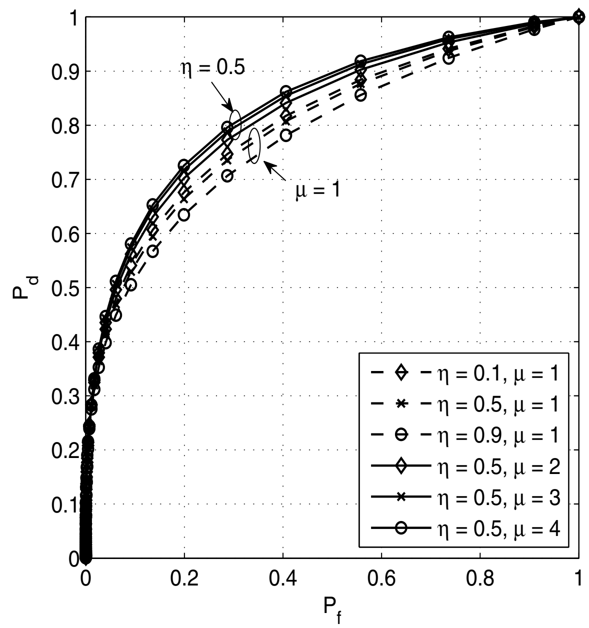

Fig. 2. P_d versus P_f for Format 2 with different η and μ values.

V. Numerical and Simulation Results

This section provides analytical and Monte-Carlo simulation results. Fig. 1 and Fig. 2 show the ROC performance (P_d versus P_f) under Format 1 and Format 2 of the $\eta - \mu$ fading model, respectively. Average SNR of the fading channel is $\bar{\gamma} = 5$ dB. Note that in the figures, numerical results are represented by lines, while simulation results are represented by discrete marks on the curves. It is clear that the numerical results match well with their simulation counterparts, confirming the accuracy of the analysis.

In Fig. 1, the energy detector shows better detection capability for higher η (with fixed μ) because the receiver receives more power through in-phase component. In Fig. 2, the energy detector shows better detection capability for lower η (with fixed η) because of low interference between in-phase and quadrature components. When μ increases, energy detector shows better performance for both formats due to the advantage of multipath effect.

Since our theoretical analysis is verified by simulation results in Fig. 1 and Fig. 2, no further simulation results are presented in the following figures.

Fig. 3 shows the ROC curves for different u values with $\eta = 0.5$, $\mu = 1$ and $\bar{\gamma} = 5$ dB. It can be seen that when u increases, the performance of the energy detector degrades. This is because the false alarm probability increases faster than the detection probability, thus leading to a lower overall detection capability. Fig. 4 shows the impact of the average SNR of the fading channel on the energy detector. As we expect, higher average SNR of the fading channel leads to better detection capability at the energy detector.

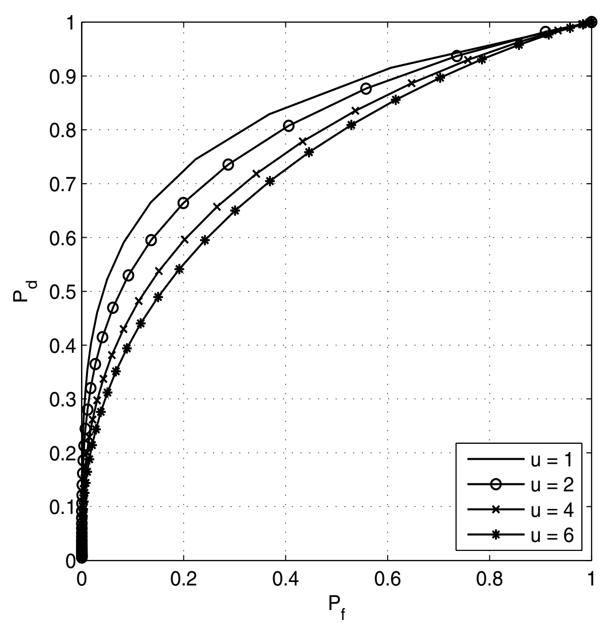

Fig. 3. P_d versus P_f for different u values

Fig. 5 shows the effect of two diversity techniques such as MRC and SLC for energy detection. The average SNR of fading channel is set as $\bar{\gamma} = 5$ dB. When the number of diversity branches is increased, ROC curves moves rapidly to the upper left corner of the ROC plot. Thus, diversity combining has major impact on detection capability. Further, MRC always outperforms SLC. The test statistics under MRC and SLC follow chi-square distributions with u and Lu degrees of freedom, respectively. The energy detector has lower detection

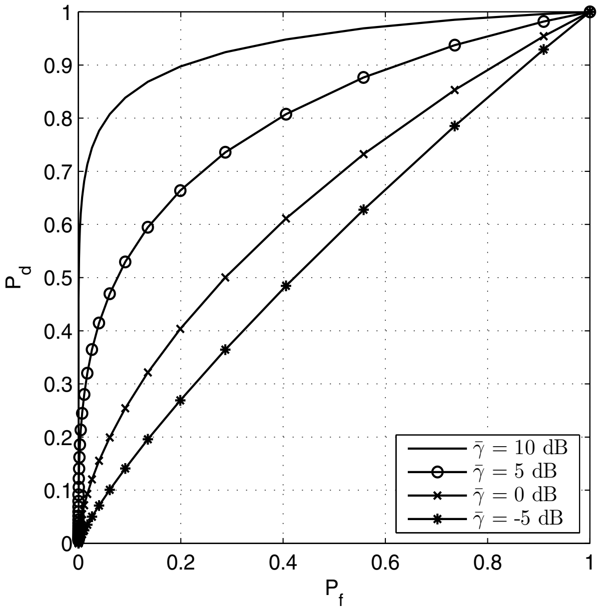

Fig. 4. P_d versus P_f for different average channel SNR ($\bar{\gamma}$) values.

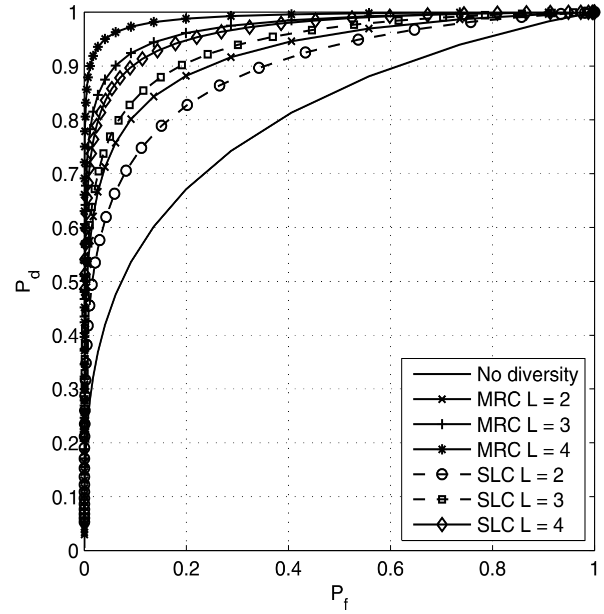

Fig. 5. P_d versus P_f for MRC and SLC diversity schemes.

capability at higher degrees of freedom as shown in Fig. 3.

VI. Conclusion

We analyze the performance of an energy detector over the $\eta - \mu$ fading channel model. The analysis derives the average detection probabilities in closed-form for cases without diversity reception and with diversity reception (MRC and SLC). It is shown that the detection probability increases when the power ratio between independent in-phase and quadrature components of the fading coefficient increases, or when the correlation coefficient between correlated in-phase and quadrature components of the fading coefficient decreases. Diversity advantage has major impact on ROC performance. MRC always outperforms SLC. The results can be used to discuss the performance of Rayleigh, Nakagami-m and Hoyt fading models as special cases of the $\eta - \mu$ fading model.

References

[1] S. Haykin, "Cognitive radio: Brain-empowered wireless communications," *IEEE J. Select. Areas Commun.*, vol. 23, no. 2, pp. 201–220, Feb. 2005.

[2] H. Jiang, L. Lai, R. Fan, and H. V. Poor, "Optimal selection of channel sensing order in cognitive radio," *IEEE Trans. Wireless Commun.*, vol. 8, no. 1, pp. 297-307, Jan. 2009.

[3] R. Fan and H. Jiang, "Channel sensing-order setting in cognitive radio networks: A two-user case," *IEEE Trans. Veh. Technol.*, vol. 58, no. 9, pp. 4997-5008, Nov. 2009.

[4] Z. Han, R. Fan, and H. Jiang, "Replacement of spectrum sensing in cognitive radio," *IEEE Trans. Wireless Commun.*, vol. 8, no. 6, pp. 2819-2826, June 2009.

[5] V. K. Bhargava and E. Hossain (eds.), *Cognitive Wireless Communication Networks*. Springer-Verlag, New York, 2007.

[6] A. Rabbachin, T. Q. S. Quek, P. C. Pinto, I. Oppermann, and M. Z. Win, "UWB energy detection in the presence of multiple narrowband interferers," in *Proc. IEEE Int. Conf. Ultra-Wideband (ICUWB)*, 2007, pp. 857–862.

[7] H. Urkowitz, "Energy detection of unknown deterministic signals," *Proceedings of the IEEE*, vol. 55, no. 4, pp. 523–531, Apr. 1967.

[8] V. I. Kostylev, "Energy detection of a signal with random amplitude," in *Proc. IEEE Int. Conf. Communications (ICC)*, 2002, pp. 1606–1610.

[9] F. F. Digham, M. S. Alouini, and M. K. Simon, "On the energy detection of unknown signals over fading channels," in *Proc. IEEE Int. Conf. Communications (ICC)*, 2003, pp. 3575–3579.

[10] ——, "On the energy detection of unknown signals over fading channels," *IEEE Trans. Commun.*, vol. 55, no. 1, pp. 21–24, Jan. 2007.

[11] S. P. Herath and N. Rajatheva, "Analysis of equal gain combining in energy detection for cognitive radio over Nakagami channels," in *Proc. IEEE Global Telecommun. Conf. (GLOBECOM)*, 2008.

[12] S. Atapattu, C. Tellambura, and H. Jiang, "Relay based cooperative spectrum sensing in cognitive radio networks," in *Proc. IEEE Global Telecommun. Conf. (GLOBECOM)*, 2009, accepted.

[13] ——, "Performance of an energy detector over channels with both multipath fading and shadowing," *IEEE Trans. Wireless Commun.*, Nov. 2009, revised.

[14] ——, "Analysis of area under the ROC curve of energy detection," *IEEE Trans. Wireless Commun.*, Oct. 2009, revised.

[15] M. D. Yacoub, "The $\eta - \mu$ distribution: A general fading distribution," in *Proc. IEEE Veh. Technol. Conf. (VTC-Fall)*, 2000, pp. 872–877.

[16] ——, "The $\kappa - \mu$ distribution and the $\eta - \mu$ distribution," *IEEE Antennas and Propagation Magazine*, vol. 49, no. 1, pp. 68–81, Feb. 2007.

[17] N. Ermolova, "Moment generating functions of the generalized $\eta - \mu$ and $\kappa - \mu$ distributions and their applications to performance evaluations of communication systems," *IEEE Commun. Lett.*, vol. 12, no. 7, pp. 502–504, July 2008.

[18] C. Tellambura, A. Annamalai, and V. K. Bhargava, "Closed form and infinite series solutions for the MGF of a dual-diversity selection combiner output in bivariate Nakagami fading," *IEEE Trans. Commun.*, vol. 51, no. 4, pp. 539–542, Apr. 2003.

[19] S. G. Krantz, *Handbook of Complex Variables, 1st Ed.* Birkhuser Boston, 1999.